INTERNATIONAL JOURNAL FOR NUMERICAL METHODS IN FLUIDS
*Int. J. Numer. Meth. Fluids* 2000; **00**:1–6 *Prepared using* fldauth.cls *[Version: 2002/09/18 v1.01]*

# Optimal control of non-isothermal viscous fluid flow

Christopher L. Cox[†], Hyesuk Lee[*], and David Szurley[‡]

*Department of Mathematical Sciences, Clemson, SC, 29634, USA*

SUMMARY

For flow inside a four-to-one contraction domain, we minimize the vortex that occurs in the corner region by controlling the heat flux along the corner boundary. The energy equation is coupled with the mass, momentum, and constitutive equations through the assumption that viscosity depends on temperature. Previous efforts in optimal control of polymeric fluid flows assume a temperature dependent Newtonian viscosity when describing the model equations, but make the simplifying assumption of a constant Newtonian viscosity when carrying out computations; we assume no such simplification for the computations. Copyright © 2000 John Wiley & Sons, Ltd.

KEY WORDS: optimal control, viscous fluid flow, vortex minimization, temperature matching

## 1. INTRODUCTION

Today's society has in great abundance products that are made from polymers: clothing made from synthetic fibers, plastic bags, food wrap, and disposable diapers are among the most common examples. It has become imperative for today's manufacturers to understand the processes used to make these products as fully as possible. Numerical simulation is a powerful tool which can be used for this purpose. The processes involve complex fluid flow of molten polymer modeled by systems of differential equations, which, along with their required initial conditions and parameters, are in general difficult to solve due to the complexity of the model equations.

We consider the four-to-one contraction domain, where a fluid is flowing through a channel whose width is suddenly reduced by three-quarters. This geometry commonly occurs in the forming 'die' for polymer fibers and films. Due to the sudden reduction in width, in the corner region a vortex appears, as in Figure 1. In this region while the polymer recirculates, it has the potential to degrade, which produces an inferior product at extrusion. Hence, we would like

[*]Correspondence to: H. Lee, Department of Mathematical Sciences, Clemson, SC, 29634, USA, E-mail: hklee@clemson.edu
[†]E-mail: clcox@clemson.edu
[‡]E-mail: szurley@clemson.edu

Contract/grant sponsor: ERC Program of the National Science Foundation through the Center for Advanced Engineering Fiber and Films at Clemson University; contract/grant number: EEC-9731680


*Received 27 April 2006*
*Revised 27 April 2006*

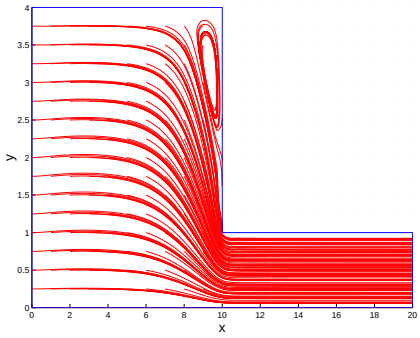


Figure 1. Typical streamlines of velocity $\mathbf{u}$.

to be able to control some parameter(s) of the flow to reduce this vortex. Also, we consider the problem of temperature matching. We wish to match a specified temperature along the outflow boundary, which represents the die exit.

Kunisch and Marduel [1] and Ito and Ravindran [2] both consider two-dimensional adjoint-based optimization for non-isothermal flow. Although the fluid in both papers is assumed to be non-isothermal, in both cases the Newtonian viscosity is independent of temperature. Ito and Ravindran consider the Boussinesq equations, and hence stress is not an unknown. The focus of that work is minimizing vortices controlling the temperature along a portion of the boundary. A cost functional is introduced where the curl of the velocity field is minimized over the domain or a portion of the domain. The authors look at the backward-facing-step channel as well as a vertical reactor. It is shown that they can reduce the $L^2$ norm of the vorticity by 46% by controlling the temperature along a portion of the boundary.

In [1] the authors also consider vortex minimization, although there are differences between [1] and [2], the first of which is the computational domain. In [1], they consider flow of a non-isothermal viscoelastic fluid (governed by the linearized Phan-Thien/Tanner model) through the four-to-one contraction domain, which is common in polymer applications. Also, they introduce two cost functionals, both of which are intended to minimize the vorticity. One minimizes the difference between the computed flow field and the flow field of a Newtonian fluid, and the other penalizes negative contributions of the velocity field to prevent recirculation. They do not assume symmetry, and hence apply one cost functional to each corner region. Using temperature as a control, they show that the vortex can be reduced, and then discuss in physical terms what has to happen to lead to a reduction in the vortex.

Like [2] and [1], we consider non-isothermal flow. However, we do not make the assumption that the Newtonian viscosity is independent of temperature; that is, the equation governing temperature is coupled to the other equations through the Newtonian viscosity.

The outline of the rest of this paper is as follows. In the next section we present the governing equations, with particular attention given to the manner in which temperature dependence is expressed. The optimization problem and the adjoint equations are defined in Section 3. Section 4 contains details of the weak formualtion of the governing equations and the computational algorithm. Numerical results for three model problems are presented in Section 5, and Section 6 contains a summary and a discussion of future work.

## 2. GOVERNING EQUATIONS

The current effort is directed towards the long term goal of optimal control of viscoelastic fluid flow. With this goal in mind, we give a brief derivation of the governing equations used in the present work. We consider fluid flowing through a bounded, connected domain $\Omega \subset \mathbb{R}^{\acute{d}}$, whose boundary we denote as $\Gamma$. Let the velocity be denoted by $\mathbf{u}$, pressure $p$, extra stress $\underline{\sigma}$, temperature $T$, and unit vectors outward and tangential to the boundary $\mathbf{n}$ and $\mathbf{t}$, respectively. Keunings [3] provides the general form of the equations governing viscoelastic fluid flows, with the assumption of incompressibility, as follows. The Cauchy stress $\underline{\pi}$ can be expressed in terms of the pressure $p$ and extra stress $\underline{\sigma}$ as

$$\underline{\pi} = -p\underline{\delta} + \underline{\sigma}, \tag{1}$$

where $\underline{\delta}$ is the identity tensor. The continuity equation takes the form

$$\nabla \cdot \mathbf{u} = 0, \tag{2}$$

and the momentum equation, assuming steady state flow with no inertial terms can be written as

$$-\nabla \cdot \underline{\pi} = \mathbf{f}, \tag{3}$$

where $\mathbf{f}$ is a body source term. Combining (1) and (3) leads to

$$-\nabla \cdot \underline{\sigma} + \nabla p = \mathbf{f}. \tag{4}$$

For viscoelastic fluid flow, the extra stress tensor is often split into solvent and polymer parts,

$$\underline{\sigma} = \underline{\sigma}_s + \underline{\sigma}_p.$$

Normally the solvent part of the extra stress is assumed to be Newtonian, i.e.

$$\underline{\sigma}_s = 2\frac{\eta_s(T)}{\eta_0(T_R)} d(\mathbf{u}), \tag{5}$$

where $\eta_s(T)$ is the solvent viscosity, $\eta_0(T_R)$ the zero-shear viscosity at a reference temperature $T_R$, and $d(\mathbf{u})$, the rate of deformation tensor, is defined as

$$d(\mathbf{u}) = \frac{1}{2}\left(\nabla\mathbf{u} + (\nabla\mathbf{u})^T\right).$$

Equation (4) then becomes

$$-\nabla \cdot \left(\underline{\sigma}_p + 2\frac{\eta_s(T)}{\eta_0(T_R)} d(\mathbf{u})\right) + \nabla p = \mathbf{f}. \tag{6}$$

The system of equations (2), (6) is closed by introducing a constitutive equation relating polymeric stress and $d(\mathbf{u})$. The constitutive model is generally nonlinear and differential or integral in nature. The Oldroyd-B model, for example, has the form

$$\underline{\sigma}_p + \lambda \underline{\sigma}_{p,(1)} = 2\eta[d(\mathbf{u}) + \lambda^* d(\mathbf{u})_{(1)}], \tag{7}$$

where $\underline{\varphi}_{(1)}$ is the upper convected derivative of the tensor $\underline{\varphi}$, $\eta$ is the total shear viscosity, i.e.,

$$\eta = \eta_s + \eta_p,$$

$\lambda$ is a relaxation time, $\lambda^* = \frac{\lambda\eta_s}{\eta}$, and $\eta_p$ is the polymeric viscosity, which could be temerature dependent. We simplify the model to a nonisothermal viscous flow but preserve the dependent variable structure of the viscoelastic case. Toward that end, we set $\lambda$ in (7) to 0 and assume that the form of the polymeric stress $\underline{\sigma}_p$ is similar to that of the solvent (5). We then have

$$\underline{\sigma}_p = 2\frac{\eta_p(T)}{\eta_0(T_R)}d(\mathbf{u}). \tag{8}$$

As in [1] and [2], we drop the viscous heating term in the energy equation, so that the steady state form of this equation is

$$-\nabla\cdot(\kappa\nabla T) + \mathbf{u}\cdot\nabla T = Q, \tag{9}$$

where $\kappa$ is a dimensionless term related to thermal conductivity and $Q$ is a heat source term.

We couple the system of equations (2), (6), and (8) by allowing both the solvent and polymeric parts of the viscosity to depend on temperature, and assume that $\eta_s$ is significantly smaller than $\eta_p$. Specifically, we introduce $\alpha_1(T)$ and $\alpha_2(T)$ and assume that an Arrhenius relationship can be used to express the dependence of viscosity on temperature [4] so that

$$\frac{\eta_p(T)}{\eta_0(T_R)} = \alpha_1(T) = A_1\exp\left(\frac{B_1}{T}\right), \tag{10}$$

and

$$\frac{\eta_s(T)}{\eta_0(T_R)} = \epsilon\alpha_2(T) = \epsilon A_2\exp\left(\frac{B_2}{T}\right), \tag{11}$$

with $\alpha_1$ and $\alpha_2$ of similar magnitude and $\epsilon$ small. In equations (10) and (11), the temperature $T$ has dimensions Kelvin. We assume further that there exist constants $\alpha_{1,min}$ and $\alpha_{2,min}$ so that

$$0 < \alpha_{1,min} \le \alpha_1(T) \le 1,$$

and

$$0 < \alpha_{2,min} \le \alpha_2(T) \le 1,$$

and that $B_1 \neq 0$.

In the rest of this paper, the polymeric stress $\underline{\sigma}_p$ will be referred to as $\underline{\sigma}$ for ease of notation. Our governing equations are then

$$\begin{aligned}
\underline{\sigma} + 2\alpha_1(T)d(\mathbf{u}) &= \underline{0} \text{ in } \Omega, &(12)\\
-\nabla\cdot[\underline{\sigma} + 2\epsilon\alpha_2(T)d(\mathbf{u})] + \nabla p &= \mathbf{f} \text{ in } \Omega, &(13)\\
\nabla\cdot\mathbf{u} &= 0 \text{ in } \Omega, &(14)\\
-\nabla\cdot(\kappa\nabla T) + \mathbf{u}\cdot\nabla T &= Q \text{ in } \Omega, &(15)
\end{aligned}$$

where the boundary conditions will be specified later. Based on [5], we refer to these equations as the modified non-isothermal Stokes-Oldroyd equations. See [6] for analysis of the solution of equations (12)-(15).

Here we relate the values for $A_i$ and $B_i$ to physical quantities and establish conditions to assure that $0 < \alpha_i(T) \le 1$. The form for the Arrhenius-type temperature shift factor is

$$a_T = \exp\left[\frac{\Delta E}{R}\left(\frac{1}{T} - \frac{1}{T_R}\right)\right],$$

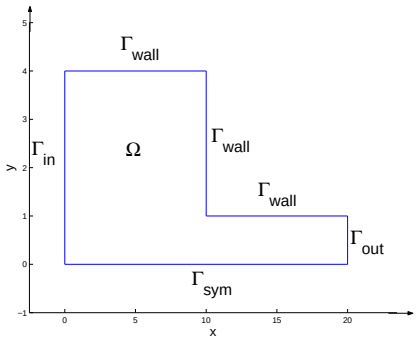


Figure 2. Computational domain $\Omega$.

where $\Delta E$ is the activation energy and $R$ the ideal gas constant, [4]. Assuming that the polymer and solvent viscosities add up to the zero-shear viscosity, (as in [7]), it follows that $\alpha_1(T) = (1-\epsilon)a_T$ and $\alpha_2(T) = a_T$. As a result, for our simplified model, we set

$$B_1 = B_2 = \tfrac{\Delta E}{R},\ A_2 = \exp\left[\tfrac{-\Delta E}{RT_R}\right], \text{ and } A_1 = (1-\epsilon)A_2$$

The constraint $0 < \alpha_i(T) \leq 1$ will be satisfied as long as the temperature of the system stays above $T_R$. This constraint can be relaxed somewhat for $T \leq T_R$ so the analytic results hold as long as there is a positive finite constant $A$ so that $0 < \alpha_i \leq A$. This condition is simple to satisfy for the application considered in this paper, i.e. flow through a fiber- or film-forming die. As shown in Figure 2, boundary $\Gamma$ is divided into four parts: the inflow boundary $\Gamma_{in}$, the wall boundary $\Gamma_{wall}$, the outflow boundary $\Gamma_{out}$, and the symmetry boundary $\Gamma_{sym}$ (so that $\Gamma = \Gamma_{in} \cup \Gamma_{wall} \cup \Gamma_{out} \cup \Gamma_{sym}$). Then the boundary conditions are as follows [7].

- Inflow boundary $\Gamma_{in}$:

$$\begin{aligned} \mathbf{u} &= \mathbf{u}_{in}, \\ T &= T_0. \end{aligned}$$

- Wall boundary $\Gamma_{wall}$:

$$\begin{aligned} \mathbf{u} &= \mathbf{0}, \\ \nabla T \cdot \mathbf{n} &= 0. \end{aligned}$$

- Outflow boundary $\Gamma_{out}$:

$$\begin{aligned} \mathbf{u} &= \mathbf{u}_{out}, \\ \nabla T \cdot \mathbf{n} &= 0. \end{aligned}$$

- Symmetry boundary $\Gamma_{sym}$:

$$\begin{aligned} \mathbf{u} \cdot \mathbf{n} &= 0, \\ \nabla T \cdot \mathbf{n} &= 0, \\ \underline{\pi} : \mathbf{nt} &= 0. \end{aligned}$$

Note that the boundary condition $\underline{\pi} : \mathbf{nt}$ on $\Gamma_{sym}$ is equivalent for the problem considered here to $\frac{\partial u_1}{\partial y} = 0$.

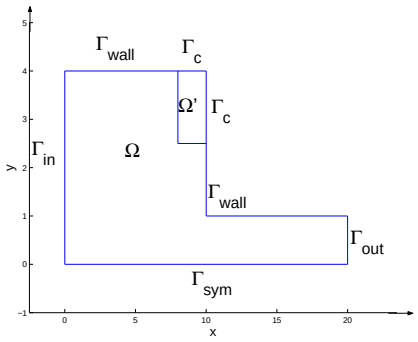


Figure 3. Domain of the control problem.

## 3. OPTIMIZATION PROBLEM AND ADJOINT EQUATIONS

As stated previously our goal is to minimize the vortex in the corner region, as shown in Figure 1, or ideally eliminate it altogether. A measure of the vortex is the curl of the velocity field. Hence, an optimization problem consists of minimizing the magnitude of the curl, e.g.,

$$\int_{\Omega} (\nabla \times \mathbf{u})^2 \, d\Omega \tag{16}$$

subject to the state equations (12)-(15). We will also consider matching a desired temperature $T^*$ along the outflow boundary. Then our optimization problem is to minimize

$$\int_{\Omega} (\nabla \times \mathbf{u})^2 \, d\Omega + \int_{\Gamma_{out}} (T - T^*)^2 d\Gamma,$$

subject to the state equations.

With the quantity that is to be minimized defined, as well as the constraints, it is now necessary to define the control variable. Similar to Kunisch et al. [1], we consider affecting the flow by a temperature boundary control. However, while the authors of [1] consider temperature $T$ along a portion of the boundary as their control, we consider controlling the heat flux over a portion of the boundary, as in [8], and similar to the condition in [2]. Specifically, we let our control $\tilde{g}$ be defined as

$$\tilde{g} = -\kappa \nabla T \cdot \mathbf{n},$$

which is applied to a subset $\Gamma_c$ of the boundary. The domain $\Omega$ for the control problem is shown in Figure 3. We now have the following conditions on the control boundary $\Gamma_c$:

$$\begin{aligned} \mathbf{u} &= \mathbf{0}, \\ -\kappa \nabla T \cdot \mathbf{n} &= \tilde{g}, \end{aligned}$$

where the quantity $\tilde{g}$ is determined by optimization.

In order to ensure that the control $\tilde{g}$ has a realistic magnitude, we introduce a penalty term. Also, we will weight the curl and temperature integrals in order to vary the extent to which each optimization condition is enforced. Define the cost functional as

$$\mathcal{J}_\delta(\mathbf{u}, p, \underline{\sigma}, T, \tilde{g}) = \frac{a}{2} \int_{\Omega'} (\nabla \times \mathbf{u})^2 \, d\Omega + \frac{\delta}{2} \int_{\Gamma_c} \tilde{g}^2 d\Gamma + \frac{1-a}{2} \int_{\Gamma_{out}} (T - T^*)^2 \, d\Gamma, \tag{17}$$

where $0 \leq a \leq 1$. Notice that in the first term on the right hand side, we only integrate over a portion of the domain $\Omega' \subset \Omega$. The penalty term has a coefficient $\delta$, which is assumed to be small.

Our optimal control problem is then to find a suitable control $\tilde{g}$ such that $\mathcal{J}_\delta$ is minimized subject to the state equations (12)-(15).

We will consider adjoint-based optimization techniques. Adjoint-based optimization methods turn a constrained optimization problem into an unconstrained one [9]. For completeness, we present the strong form of the adjoint equations, their boundary conditions, and the optimality condition. Motivation for the derivation of the equations and boundary equations is given in the next section. The adjoint equations are:

$$\begin{aligned}
\underline{\gamma} + d(\boldsymbol{\mu}) &= \underline{0}, \\
2\nabla \cdot (\alpha_1(T)\underline{\gamma}) - 2\epsilon\nabla \cdot (\alpha_2(T)d(\boldsymbol{\mu})) + \nabla\xi + \nabla T\Phi &= -a\nabla \times \nabla \times \mathbf{u}, \\
\nabla \cdot \boldsymbol{\mu} &= 0, \\
-\nabla \cdot (\kappa\nabla\Phi) - \mathbf{u} \cdot \nabla\Phi + \frac{2B_1}{T^2}\alpha_1(T)d(\mathbf{u}) : \underline{\gamma} - \frac{2\epsilon B_2}{T^2}\alpha_2(T)d(\mathbf{u}) : d(\boldsymbol{\mu}) &= 0,
\end{aligned}$$

where $\underline{\gamma}$, $\boldsymbol{\mu}$, $\xi$, and $\Phi$ are the adjoint stress, velocity, pressure, and temperature, respectively. Note that the adjoint equations are linear in the adjoint variables.

The boundary conditions for the adjoint equations are as follows.

- Inflow boundary $\Gamma_{in}$:

$$\begin{aligned}
\boldsymbol{\mu} &= \mathbf{0}, \\
\Phi &= 0.
\end{aligned}$$

- Wall boundary $\Gamma_{wall}$:

$$\begin{aligned}
\boldsymbol{\mu} &= \mathbf{0}, \\
\frac{2\epsilon B_2}{T^2}\alpha_2(T)d(\mathbf{u}) \cdot \boldsymbol{\mu} \cdot \mathbf{n} + \kappa\nabla\Phi \cdot \mathbf{n} &= 0.
\end{aligned}$$

- Outflow boundary $\Gamma_{out}$:

$$\begin{aligned}
\boldsymbol{\mu} &= \mathbf{0}, \\
\frac{2\epsilon B_2}{T^2}\alpha_2(T)d(\mathbf{u}) \cdot \boldsymbol{\mu} \cdot \mathbf{n} + \kappa\nabla\Phi \cdot \mathbf{n} + \Phi\mathbf{u} \cdot \mathbf{n} + (1-a)(T - T^*) &= 0.
\end{aligned}$$

- Symmetry boundary $\Gamma_{sym}$:

$$\begin{aligned}
\boldsymbol{\mu} &= \mathbf{0}, \\
\frac{2\epsilon B_2}{T^2}\alpha_2(T)d(\mathbf{u}) \cdot \boldsymbol{\mu} \cdot \mathbf{n} + \kappa\nabla\Phi \cdot \mathbf{n} &= 0.
\end{aligned}$$

- Control boundary $\Gamma_c$:

$$\begin{aligned}
\boldsymbol{\mu} &= \mathbf{0}, \\
\frac{2\epsilon B_2}{T^2}\alpha_2(T)d(\mathbf{u}) \cdot \boldsymbol{\mu} \cdot \mathbf{n} + \kappa\nabla\Phi \cdot \mathbf{n} &= 0.
\end{aligned}$$

Finally, the optimality condition is found to be

$$\tilde{g} + \frac{1}{\delta}\Phi = 0.$$

## 4. FINITE ELEMENT FORMULATION

We develop the variational formulation of the modified non-isothermal Stokes-Oldroyd equations and the associated adjoint equations. Let $H^1(\Omega)$ be the standard Sobolev space with respect to a domain $\Omega$. Let $||\cdot||_1$ and $(\cdot,\cdot)_\Omega$ be the norm and inner product for $H^1(\Omega)$, respectively. Finally, let $\mathbf{H}^1(\Omega)$ be the corresponding Sobolev space of vector-valued functions in $\mathbb{R}^{\acute{d}}$. We have the following approximation spaces:

$$\begin{gathered}\text{Velocity Space} : \mathbf{X} := \mathbf{H}^1(\Omega),\\ \text{Pressure Space} : P := L^2(\Omega),\\ \text{Stress Space} : \mathbf{\Sigma} := \left(L^2(\Omega)\right)^{\acute{d}\times\acute{d}} \cap \{\underline{\tau} = (\tau_{ij}) : \tau_{ij} = \tau_{ji}, \tau_{ij} \in L^2(\Omega)\},\\ \text{Temperature Space} : E := H^1(\Omega).\end{gathered}$$

Notice that the velocity and pressure spaces, $\mathbf{X}$ and $P$ respectively, satisfy the $inf - sup$ condition [10, 11]

$$\inf_{q\in P}\sup_{\mathbf{v}\in\mathbf{X}} \frac{(q, \nabla\cdot\mathbf{v})}{||q||_0||\mathbf{v}||_1} \geq \beta > 0.$$

Now define the bilinear and trilinear forms

$$\begin{aligned} b(p,\mathbf{v}) &= -\int_\Omega p \ \ \nabla\cdot\mathbf{v} \quad d\Omega,\\ e(T,S) &= \int_\Omega \nabla T\cdot\nabla S \quad d\Omega,\\ c(\mathbf{u},T,S) &= \int_\Omega \mathbf{u}\cdot\nabla TS \quad d\Omega. \end{aligned}$$

We have the property that $c(\mathbf{u},T,T) = 0$ if $\mathbf{u} = \mathbf{0}$ on $\Gamma$ and $\nabla\cdot\mathbf{u} = 0$. With these forms defined, the weak form of the modified non-isothermal Stokes-Oldroyd equations is to find $(\mathbf{u},p,\underline{\sigma},T) \in \mathbf{X}\times P\times\mathbf{\Sigma}\times E$ so that

$$\begin{aligned} (\underline{\sigma},\underline{\tau})_\Omega - 2(\alpha_1(T)d(\mathbf{u}),\underline{\tau})_\Omega &= 0 \qquad \forall\underline{\tau}\in\mathbf{\Sigma}, &(18)\\ (\underline{\sigma},d(\mathbf{v}))_\Omega + 2\epsilon(\alpha_2(T)d(\mathbf{u}),d(\mathbf{v}))_\Omega + b(p,\mathbf{v}) &= (\mathbf{f},\mathbf{v})_\Omega \qquad \forall\mathbf{v}\in\mathbf{X}, &(19)\\ b(q,\mathbf{u}) &= 0 \qquad \forall q\in P, &(20)\\ \kappa e(T,S) + c(\mathbf{u},T,S) - \kappa(\nabla T\cdot\mathbf{n},S)_{\Gamma_c} &= (Q,S)_\Omega \qquad \forall S\in E, &(21)\end{aligned}$$

and the corresponding boundary conditions are satisfied. The heat flux $\kappa(\nabla T\cdot\mathbf{n},S)_{\Gamma_c}$ arises from Green's theorem when obtaining the weak form of the energy equation. If the heat flux on $\Gamma_c$ is given as

$$\tilde{g} = -\kappa\nabla T\cdot\mathbf{n}, \tag{22}$$

then the weak form of the energy equation becomes

$$\kappa e(T,S) + c(\mathbf{u},T,S) = (Q,S)_\Omega - (\tilde{g},S)_{\Gamma_c} \quad \forall S\in E. \tag{23}$$

We now present the motivation for the adjoint equations. We'll describe the general framework and then apply it to our problem. Let $\phi$ denote the state variables, $g$ the control

variable(s), $F(\phi, g)$ the state equations, $\mathcal{J}$ the cost functional, and $\zeta$ the adjoint variables. The Lagrangian is defined as

$$\mathcal{L}(\phi, g, \zeta) = \mathcal{J} - \zeta^* F(\phi, g).$$

Then the unconstrained optimization problem is to find states $\phi$, control $g$, and adjoint variables $\zeta$ so that the Lagrangian is rendered stationary. The first order necessary conditions yield the optimality system from which we can determine the optimal states $\phi$ and control $g$. Consider taking the Fréchet derivative with respect to the state variables, adjoint variables, and control. We then have the following relationships:

$$\begin{aligned} \tfrac{\partial \mathcal{L}}{\partial \phi} = 0 &\Rightarrow \text{Adjoint equations,} \\ \tfrac{\partial \mathcal{L}}{\partial \zeta} = 0 &\Rightarrow \text{State equations,} \\ \tfrac{\partial \mathcal{L}}{\partial g} = 0 &\Rightarrow \text{Optimality condition(s).} \end{aligned}$$

With $\mathcal{J} = \mathcal{J}_\delta$ in (17), $F$ as in (12)-(15) and the Dirichlet boundary conditions for the state equations, the Lagrangian is the following equation:

$$\begin{aligned} \mathcal{L}(\mathbf{u}, p, \underline{\sigma}, T, \tilde{g}, \boldsymbol{\mu}, \xi, \underline{\gamma}, \Phi, \rho, \lambda_i) \quad = \quad & \frac{a}{2}\int_{\Omega'} (\nabla \times \mathbf{u})^2 \, d\Omega + \frac{\delta}{2}\int_{\Gamma_c} \tilde{g}^2 d\Gamma \\ & + \frac{1-a}{2}\int_{\Gamma_{out}} (T - T^*)^2 d\Gamma + \int_\Omega [\underline{\sigma} - 2\alpha_1(T) d(\mathbf{u})] : \underline{\gamma} d\Omega \\ & + \int_\Omega [-\nabla \cdot (\underline{\sigma} + 2\epsilon\alpha_2(T) d(\mathbf{u})) + \nabla p - \mathbf{f}] \cdot \boldsymbol{\mu} d\Omega \\ & + \int_\Omega (-\nabla \cdot \mathbf{u}) \xi d\Omega + \int_\Omega [-\nabla \cdot (\kappa \nabla T) + \mathbf{u} \cdot \nabla T - Q] \, \Phi d\Omega \\ & + \int_{\Gamma_c} \tilde{g} \Phi d\Gamma + \int_{\Gamma_{in}} (\mathbf{u} - \mathbf{u}_{in}) \lambda_1 d\Gamma + \int_{\Gamma_{wall} \cup \Gamma_c} (\mathbf{u} - \mathbf{0}) \lambda_2 d\Gamma \\ & + \int_{\Gamma_{sym}} (\mathbf{u} \cdot \mathbf{n} - 0) \lambda_3 d\Gamma + \int_{\Gamma_{in}} (T - T_0) \lambda_4 d\Gamma, \end{aligned}$$

where the $\lambda_i$'s are the adjoint multipliers associated with the boundary conditions. Taking the Fréchet derivative of the Lagrangian with respect to the state variables, and then applying Green's theorem will result in the weak form of the adjoint equations and their boundary conditions. Enforcing the domain integrals to be zero will yield the adjoint equations, and enforcing the boundary integrals to be zero will yield their boundary conditions. In particular, setting $\frac{\partial \mathcal{L}}{\partial \underline{\sigma}} = 0$ will yield the adjoint constitutive equation:

$$(\underline{\gamma}, \underline{\tau})_\Omega + (d(\boldsymbol{\mu}), \underline{\tau})_\Omega = 0 \quad \forall \underline{\tau} \in \boldsymbol{\Sigma}.$$

Taking the derivative of the Lagrangian with respect to velocity will give the adjoint momentum equation:

$$\begin{aligned} -2(\alpha_1(T)\underline{\gamma}, d(\mathbf{v}))_\Omega + 2\epsilon(\alpha_2(T) d(\boldsymbol{\mu}), d(\mathbf{v}))_\Omega & \\ + b(\xi, \mathbf{v}) + c(\mathbf{v}, T, \Phi) \quad = \quad & -a(\nabla \times \mathbf{u}, \nabla \times \mathbf{v})_{\Omega'} \quad \forall \mathbf{v} \in \mathbf{X}. \end{aligned}$$

The adjoint incompressibility condition is obtained by setting $\frac{\partial \mathcal{L}}{\partial p} = 0$:

$$b(q, \boldsymbol{\mu}) = 0 \quad \forall q \in P.$$

Finally, taking the derivative with respect to temperature gives the adjoint energy equation:

$$\kappa e(\Phi,S)-c(\mathbf{u},\Phi,S)+2\int_\Omega \frac{B_1}{T^2}\alpha_1(T)d(\mathbf{u}):\underline{\gamma}Sd\Omega$$
$$-2\epsilon\int_\Omega \frac{B_2}{T^2}\alpha_2(T)d(\mathbf{u}):d(\boldsymbol{\mu})Sd\Omega \quad = \quad -(1-a)\int_{\Gamma_{out}}(T-T^*)Sd\Gamma \quad \forall S\in E.$$

The weak form of the optimality condition is found by setting $\frac{\partial\mathcal{L}}{\partial\tilde{g}}=0$. We obtain

$$(\tilde{g},S)_{\Gamma_c}=-\frac{1}{\delta}(\Phi,S)_{\Gamma_c},$$

for all $S\in H^1(\Gamma)$.

We will use the finite element method to approximate the solution to the state equations (18)-(20), (23) and the adjoint equations. Suppose $T_h$ is a triangulation of the domain $\Omega$ such that $\bar{\Omega}=\{\cup K : K\in T_h\}$; i.e., $K$ is an element of the triangulation. Further suppose that there exist positive constants $c_1$ and $c_2$ such that

$$c_1 h\le h_K\le c_2\rho_K,$$

where $h_K$ is the diameter of $K$, $\rho_K$ is the diameter of the greatest ball included in $K$, and $h=\max_{K\in T_h}h_K$. Denote the space of polynomials of degree less than or equal to $k$ on $K\in T_h$ by $P_k(K)$. To approximate the strong solution $(\mathbf{u},p,\underline{\sigma},T)$, we define the following finite-element spaces in $\mathbb{R}^{\acute{d}}$.

$$\begin{aligned}
\mathbf{X}^h &:= \{\mathbf{v}\in\mathbf{X}\cap(C^0(\bar{\Omega}))^{\acute{d}} : \mathbf{v}|_K\in P_2(K),\forall K\in T_h\},\\
P^h &:= \{q\in P\cap C^0(\bar{\Omega}) : q|_K\in P_1(K),\forall K\in T_h\},\\
\mathbf{\Sigma}^h &:= \{\underline{\tau}\in\mathbf{\Sigma} : \underline{\tau}|_K\in P_1(K),\forall K\in T_h\},\\
E^h &:= \{S\in E\cap C^0(\bar{\Omega}) : S|_K\in P_2(K),\forall K\in T_h\}.
\end{aligned}$$

We are using continuous piecewise quadratic elements for velocity and temperature, continuous piecewise linear elements for pressure, and discontinuous piecewise linear elements for stress. We use discontinuous elements in anticipation of applying this method to equations with more complex constitutive models which require a form of upwinding in the numerical approximation [12]. Analogous to the continuous function spaces, the discrete spaces $\mathbf{X}^h$ and $P^h$ satisfy the discrete $inf-sup$ condition [11]:

$$\inf_{q^h\in P^h}\sup_{\mathbf{v}^h\in\mathbf{X}^h}\frac{b(q^h,\mathbf{v}^h)}{||q^h||_0||\mathbf{v}^h||_1}\ge\beta>0.$$

Our discrete problem for the state variables is then to find $(\mathbf{u}^h,p^h,\underline{\sigma}^h,T^h)\in(\mathbf{X}^h,P^h,\mathbf{\Sigma}^h,E^h)$ such that

$$\begin{aligned}
(\underline{\sigma}^h,\underline{\tau}^h)_\Omega-2(\alpha_1(T^h)d(\mathbf{u}^h),\underline{\tau}^h)_\Omega &= 0 \qquad \forall\underline{\tau}^h\in\mathbf{\Sigma}^h, \quad (24)\\
(\underline{\sigma}^h,d(\mathbf{v}^h))_\Omega+2\epsilon(\alpha_2(T^h)d(\mathbf{u}^h),d(\mathbf{v}^h))_\Omega+b(p^h,\mathbf{v}^h) &= (\mathbf{f},\mathbf{v}^h)_\Omega \qquad \forall\mathbf{v}^h\in\mathbf{X}^h, \quad (25)\\
b(q^h,\mathbf{u}^h) &= 0 \qquad \forall q^h\in P^h, \quad (26)\\
\kappa e(T^h,S^h)+c(\mathbf{u}^h,T^h,S^h) &= (Q,S^h)_\Omega \\
&\quad -(\tilde{g},S^h)_{\Gamma_c} \quad \forall S^h\in E^h, \quad (27)
\end{aligned}$$

and the corresponding boundary conditions are satisfied.

To solve the unconstrained optimization problem, we use the method of steepest descent, [9]. The gradient method step is

$$\tilde{g}^{(n+1)} = \tilde{g}^{(n)} - \frac{\nu}{\delta}\frac{\partial \mathcal{J}_\delta}{\partial \tilde{g}},$$

where $\nu$ is a (constant) step size. By calculating $\frac{\partial \mathcal{J}_\delta}{\partial \tilde{g}}$, we find that the update for the control $\tilde{g}$ is

$$\tilde{g}^{(n+1)} = (1-\nu)\tilde{g}^{(n)} - \frac{\nu}{\delta}\Phi^{(n)}.$$

We will use the following steps when solving the optimal control problem. Initialize the control variable $\tilde{g}^{(0)}$. For $n = 0, 1, \ldots$

1. Solve the state equations to obtain the state solution $(\mathbf{u}^{(n)}, p^{(n)}, \underline{\sigma}^{(n)}, T^{(n)})$.
2. Solve the adjoint equations to obtain the adjoint solution $(\boldsymbol{\mu}^{(n)}, \xi^{(n)}, \underline{\gamma}^{(n)}, \Phi^{(n)})$.
3. Evaluate the cost functional $\mathcal{J}_\delta(\mathbf{u}^{(n)}, p^{(n)}, \underline{\sigma}^{(n)}, T^{(n)}, \tilde{g}^{(n)})$ (optional).
4. Update the control via $\tilde{g}^{(n+1)} = (1-\nu)\tilde{g}^{(n)} + \frac{\nu}{\delta}\Phi^{(n)}$.
5. Test for convergence, either by checking the optimality condition $\tilde{g}^{(n)} + \frac{1}{\delta}\Phi^{(n)} = 0$, or a maximum change in the control $||\tilde{g}^{(n+1)} - \tilde{g}^{(n)}||_\infty$.
6. Repeat all steps until convergence is attained.

Newton's method is used in Step 1 due to the nonlinear forms present in the state system. The step size $\frac{\nu}{\delta}$ for the gradient method is chosen appropriately so that a favorable convergence in the iterates is observed. A more rigorous method for determining the step size, icluding adaptivity, would improve convergence properties. Such an approach is beyond the scope of the current work.

## 5. NUMERICAL RESULTS

In this section, we cosider three scenarios: the problems of vortex minimization and temperature matching, and the combination of those two problems. In all three problems, we have the following characteristics. The dimensions of the channel before the contraction are $\{(x, y) : 0 \le x \le 10, 0 \le y \le 4\}$, while after the contraction the dimensions become $\{(x, y) : 10 \le x \le 20, 0 \le y \le 1\}$. The computational mesh is shown in Figure 4. A more refined mesh was considered, but it was determined that the solution is not appreciably affected. Recall that the cost functional has the form (17), where $\Omega' \subset \Omega$ and $a \in [0, 1]$. The boundary segments that comprise $\Gamma_c$ were determined so that the vortex is contained within the rectangle defined by these boundary segments. For the conditions in this work, it sufficed to let $\Gamma_c = \{(x, y)|8 \le x \le 10, y = 4\} \cup \{(x, y)|x = 10, 2.5 \le y \le 4\}$. The region $\Omega'$ is $\{(x, y) : 8 \le x \le 10, 2.5 \le y \le 4\}$. Both the state pressure $p$ and the adjoint pressure $\xi$ are only determined up to a constant. For uniqueness, they are set to zero at the point $(20, 0)$. Also, we assume that the desired outflow temperature $T^*$ is constant along $\Gamma_{out}$. For future

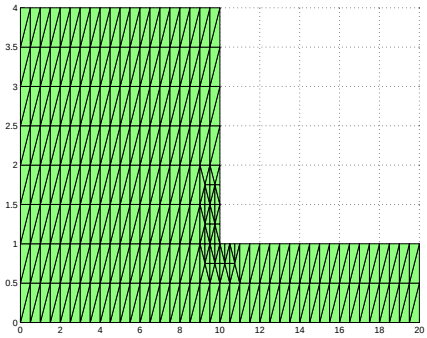


Figure 4. Computational mesh used for the FEM.

Table I. Parameter values.

| $Q$ | $T_R$ | $A_1$ | $A_2$ | $B_1$ | $B_2$ | $\epsilon$ | $\delta$ |
|---|---|---|---|---|---|---|---|
| 0 | 450K | $1.013 * 10^{-14}$ | $1.014 * 10^{-14}$ | 14500 | 14500 | 0.001 | 0.00005 |

reference, define the quadratic forms $\mathcal{I}_1$ and $\mathcal{I}_2$ as

$$\begin{aligned} \mathcal{I}_1 &= \frac{a}{2}\int_{\Omega'} (\nabla \times \mathbf{u})^2 \, d\Omega, \\ \mathcal{I}_2 &= \frac{1-a}{2}\int_{\Gamma_{out}} (T - T^*)^2 d\Gamma. \end{aligned}$$

*5.1. Vortex minimization*

We will consider the problem of minimizing the vortex in the four-to-one contraction domain. Here we consider the case where $a = 1$, i.e., we concentrate on minimizing the vortex and ignore matching the temperature along $\Gamma_{out}$. In this and all subsequent examples we set the source term $\mathbf{f}$ to zero, and assign the other parameter values as given in Table I. For this first case, we set

$$\nu = 0.05.$$

The definitions of $A_i$ and $B_i$ lead to typical zero-shear viscosity profiles for $\alpha_1(T)$ and $\alpha_2(T)$ [13]. Also, notice that the step size for the gradient method is $\frac{\nu}{\delta} = 1000$. The optimal control code ran for 153 iterations before the convergence criterion was met. The results of the run are summarized in Table II. We are able to reduce the vortex by controlling the heat flux across the boundary. We can also compare plots of the streamlines for the uncontrolled and controlled flows. These are shown in Figure 5. We are able to reduce the value of the integral by 80.6%, and it is apparent from these plots that the remaining vortex is significantly weaker than in the uncontrolled flow.

Recall that the control affects the solution of the state equations through the addition of the inner product $-(\tilde{g}, S)_{\Gamma_c}$ in the energy equation. Hence, a positive value for $\tilde{g}$ yields a heat sink

Table II. Results of the vortex minimization run.

| Iteration | $\mathcal{I}_1$ |
|---|---|
| 1 | 1.2667 |
| 2 | 1.2220 |
| 3 | 1.1750 |
| 4 | 1.1268 |
| 5 | 1.0780 |
| 6 | 1.0290 |
| 7 | 0.9796 |
| 8 | 0.9288 |
| 9 | 0.8747 |
| 10 | 0.8147 |
| 11 | 0.7462 |
| 12 | 0.6695 |
| ⋮ | ⋮ |
| 151 | 0.2461 |
| 152 | 0.2461 |
| 153 | 0.2461 |

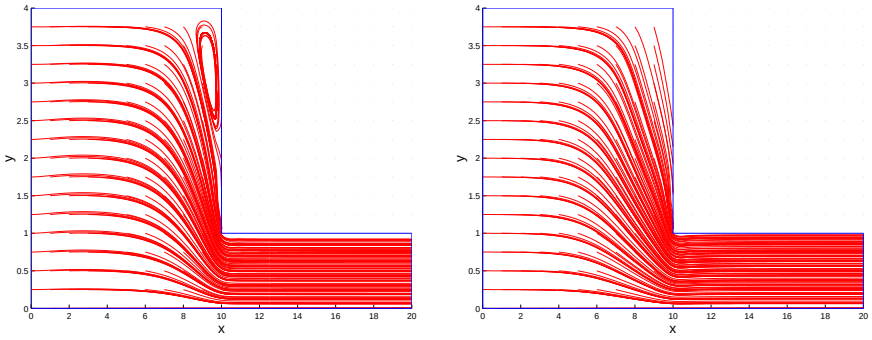


(a) Uncontrolled flow (b) Controlled flow

Figure 5. Comparison of streamlines after 153 iterations of the control algorithm.

along $\Gamma_c$, and a negative value of $\tilde{g}$ yields a heat source along $\Gamma_c$. We see that we need to cool on $\Gamma_c$ to reduce the vortex. Figure 6 contains the profile of $\tilde{g}$ as computed in this example.

### *5.2. Temperature matching*

Now we consider the case when $a = 0$, or we simply would like to match a desired temperature $T^*$ at the outflow boundary $\Gamma_{out}$. For this run, we set $\nu = 0.005$. Here notice that the step size for the gradient method is $\frac{\nu}{\delta} = 100$. Furthermore, we decide to match a desired temperature of $T^* = 550$K from an initial temperature of $T_0 = 540$K. Define $\bar{T}_f$ to be the nodal average of $T$ along $\Gamma_{out}$. The results are in Table III. The integral $\mathcal{I}_3$ strictly decreases, which means

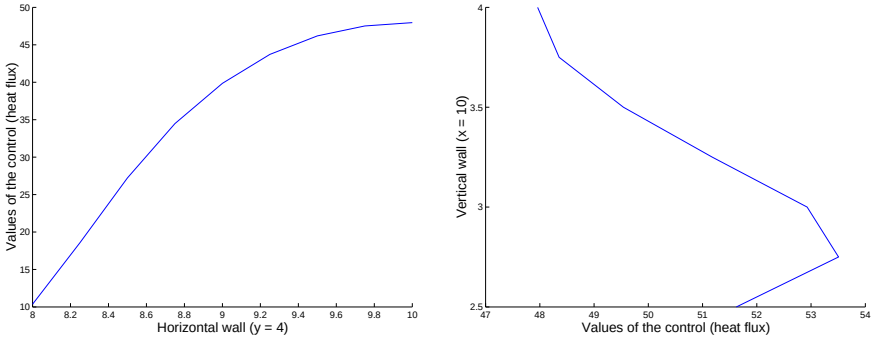


(a) Horizontal wall (b) Vertical wall

Figure 6. Profile of the control $\tilde{g}$.

Table III. Results of the temperature matching run.

| Iteration | $\mathcal{I}_2$ | $\bar{T}_f$ |
|---|---|---|
| 1 | 50.0 | 540.0 |
| 2 | 6.39 | 553.57 |
| 3 | 0.92 | 548.64 |
| 4 | 0.10 | 550.44 |
| 5 | 0.02 | 549.79 |
| 6 | $3.55 * 10^{-4}$ | 550.03 |
| 7 | $1.79 * 10^{-3}$ | 549.94 |
| 8 | $4.13 * 10^{-4}$ | 549.97 |
| 9 | $7.99 * 10^{-4}$ | 549.96 |
| 10 | $6.44 * 10^{-4}$ | 549.96 |
| 11 | $6.98 * 10^{-4}$ | 549.96 |
| 12 | $6.78 * 10^{-4}$ | 549.96 |
| 13 | $6.86 * 10^{-4}$ | 549.96 |
| 14 | $6.83 * 10^{-4}$ | 549.96 |

that as we iterate, we get closer to matching $T^*$ along $\Gamma_{out}$. We may also consider the profile of the control $\tilde{g}$. The computed control is presented in Figure 7. The negative values of $\tilde{g}$ mean that we heat along $\Gamma_c$. The heating in this case tends to increase the magnitude of the vortex. In this case, the quadratic form $\mathcal{I}_1$ will increase due to the addition of heat.

### *5.3. Combination of problems*

We have shown that we are able to minimize the vortex and match a desired outflow temperature separately. In this section we attempt to minimize both subfunctionals at the same time. Thus, we let $a = \frac{1}{2}$. We consider the case where the matching temperature is

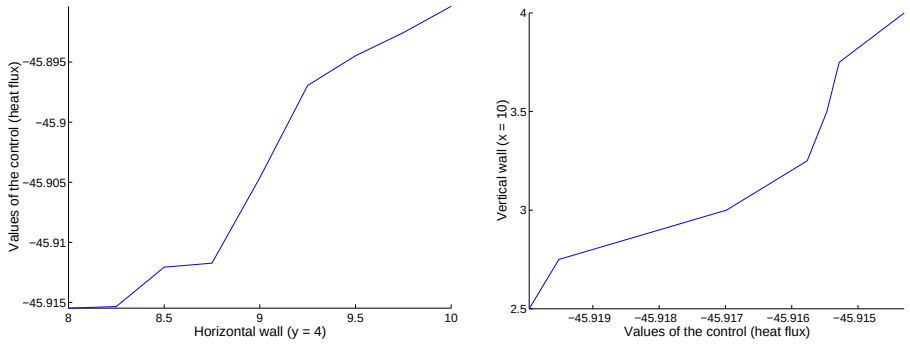


(a) Horizontal wall (b) Vertical wall

Figure 7. Profile of the control $\tilde{g}$ for the temperature matching case.

Table IV. Cost functional values for when $T^* < T_0$.

| Iteration | $\mathcal{J}_\delta$ | $\mathcal{I}_1$ | $\mathcal{I}_2$ |
|---|---|---|---|
| 1 | 25.63 | 0.63 | 25.0 |
| 2 | 11.30 | 0.43 | 10.85 |
| 3 | 5.04 | 0.32 | 4.66 |
| 4 | 2.32 | 0.23 | 1.99 |
| 5 | 1.15 | 0.18 | 0.85 |
| 6 | 0.65 | 0.14 | 0.37 |
| 7 | 0.44 | 0.12 | 0.16 |

smaller than the temperature on the inflow boundary, i.e., $T^* < T_0$. For this case,

$$\begin{aligned} \nu &= 0.0025, \\ T^* &= 530, \\ T_0 &= 540. \end{aligned}$$

The step size for the gradient method is $\frac{\nu}{\delta} = 50$. We only summarize the results of the first seven iterates. They are in Table IV. We are able to minimize both subfunctionals $\mathcal{I}_1$ and $\mathcal{I}_3$. In order to match the desired temperature, we are required to remove heat through $\Gamma_c$ which in turn reduces the vortex. We consider the profile of the control $\tilde{g}$ along the horizontal and vertical walls in this case. The profiles are presented in Figure 8.

## 6. CONCLUSIONS AND FUTURE WORK

The main thrust of this research is to apply optimal control techniques to equations modeling fluid flows related to polymer processing. Specifically, we considered fluid flow through a four-to-one contraction domain, where a vortex is generated near the corner region of the

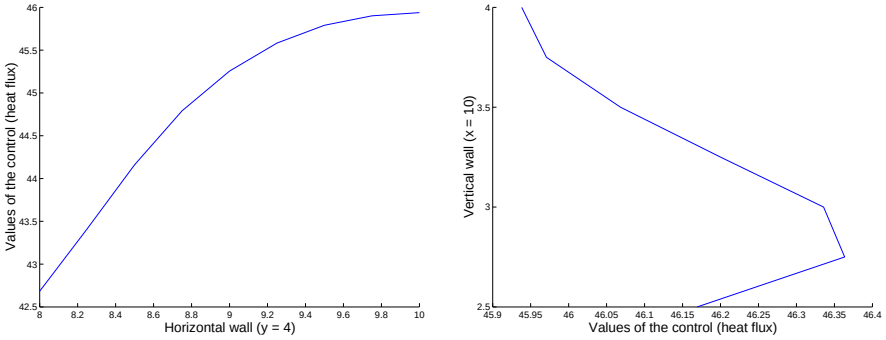


(a) Horizontal wall (b) Vertical wall

Figure 8. Profile of the control $\tilde{g}$ for when $T^* < T_0$.

contraction. Within this vortex, the polymer will recirculate for some time before being released, and may degrade. This leads to an inferior product upon extrusion. In addition to the vortex minimization problem, we looked at temperature matching along the outflow boundary. The control in each case was the heat flux across the boundary in the corner region. For the single problem of vortex minimization, we found that a combination of heating and cooling reduces the vortex. For the separate problem of temperature matching, we were able to match a specified outflow temperature $T^*$ from an initial temperature of $T_0$.

We then considered a combination of the problems. We found that we are able to minimize both the vortex and the temperature difference along the outflow boundary in the case where $T^* < T_0$. This was attained by removing heat from the system along the control boundary $\Gamma_c$.

There are many directions that we could pursue based upon this research. The first is to move on to more advanced constitutive models. Recall that the modified non-isothermal Stokes-Oldroyd equations were designed with two viscosity functions $\alpha_1(T)$ and $\alpha_2(T)$. The equations were designed in this manner with the ultimate goal of implementing a viscoelastic constitutive model in mind. In turn, we could also progress to three-dimensional flows.

In addition to the increase in complexity of the equations and advancing in spatial dimension, there are a couple of other directions we could consider. As we have only considered the flow up to the extrusion point, it would be interesting to extend the domain to include the free surface region where the fluid cools and the draw ratio is large. Optimization and control for the problem of die swell is of strong interest to industry [14]. Other optimization problems could be considered as well, such as shape optimization, to determine an optimal geometry for the interior flow domain.

## ACKNOWLEDGEMENTS

The authors gratefully acknowledge the support of the ERC Program of the National Science Foundation through the Center for Advanced Engineering Fiber and Films at Clemson University, which partially funded this research under grant number EEC-9731680.

## REFERENCES


1. Kunisch K, Marduel X. Optimal control of non-isothermal viscoelastic fluid flow. *Journal of Non-Newtonian Fluid Mechanics* 2000; **88**:261–301.
2. Ito K, Ravindran S. Optimal control of thermally convected fluid flows. *SIAM Journal of Scientific Computing* 2000; **19**(6):1847–1869.
3. Keunings R. Simulation of viscoelastic fluid flow. In *Fundamentals of Computer Modeling for Polymer Processing,* Tucker III C (ed). Carl Hanser Verlag, 1989; 402–470.
4. Bird R, Armstrong R, Hassager O. *Dynamics of Polymeric Liquids, Volume One.* John Wiley & Sons, 1987.
5. Baranger J, Sandri D. A formulation of Stoke's problem and the linear elasticity equations suggested by the Oldroyd model for viscoelastic flow. *Mathematical Modelling and Numerical Analysis* 1992; **26**:331–345.
6. Cox CL, Lee H, Szurley D. Finite element approximation of the non-isothermal Stokes-Oldroyd equations. To appear in *International Journal of Numerical Analysis and Modeling.*
7. Joo Y, Sun J, Smith M, Armstrong R, Brown R, Ross R. Two-dimensional numerical analysis of non-isothermal melt spinning with and without phase transition. *Journal of Non-Newtonian Fluid Mechanics* 2002; **102**:37–70.
8. Gunzburger M, Hou L, Svobodny T. Heating and cooling control of temperature distributions along boundaries of flow domains. *Journal of Mathematical Systems, Estimation, and Control* 1993; **3**(2):147–172.
9. Bazaraa M, Sherali H, Shetty C. *Nonlinear Programming.* John Wiley & Sons, 1993.
10. Brenner S, Scott L. *The Mathematical Theory of Finite Element Methods.* Springer-Verlag, 1996.
11. Girault V, Raviart P. *Finite Element Approximation of the Navier-Stokes Equations.* Springer-Verlag, 1979.
12. Baaijens F. An iterative solver for the DEVSS/DG method with application to smooth and non-smooth flows of the upper convected Maxwell fluid. *Journal of Non-Newtonian Fluid Mechanics* 1998; **75**:119–138.
13. Baird D, Collais D. *Polymer Processing.* John Wiley & Sons, 1998.
14. Denn M. Issues in viscoelastic fluid mechanics. *Annual Review of Fluid Mechanics* 1990; **75**:13–34.